

Penetration of surface effects on structural relaxation and particle hops in glassy films

Qiang Zhai,¹ Hai-Yao Deng,² Xin-Yuan Gao,³ Leo S.I. Lam,⁴ Sen Yang,^{1, a)} Ke Yan,^{5, b)} and Chi-Hang Lam^{6, c)}

¹⁾MOE Key Laboratory for Nonequilibrium Synthesis and Modulation of Condensed Matter, School of Physics, Xi'an Jiaotong University, Xi'an, Shaanxi, 710049, China

²⁾School of Physics and Astronomy, Cardiff University, 5 The Parade, Cardiff CF24 3AA, Wales

³⁾Department of Physics, The Chinese University of Hong Kong, Shatin, New Territories, Hong Kong, China

⁴⁾Department of Mechanical Engineering, Hong Kong Polytechnic University, Hong Kong, China

⁵⁾School of Mechanical Engineering, Xi'an Jiaotong University, Xi'an, Shaanxi, 710049, China

⁶⁾Department of Applied Physics, Hong Kong Polytechnic University, Hong Kong, China

(Dated: 17 June 2025)

A free surface induces enhanced dynamics in glass formers. We study the dynamical enhancement of glassy films with a distinguishable-particle lattice model of glass free of elastic effects. We demonstrate that the thickness of the surface mobile layer depends on temperature differently under different definitions, although all are based on local structure relaxation rate. The rate can be fitted to a double exponential form with an exponential-of-power-law tail. Our approach and results exclude elasticity as the unique mechanism for the tail. Layer-resolved particle hopping rate, potentially a key measure for activated hopping, is also studied but it exhibits much shallower surface effects.

I. INTRODUCTION

It is well known that a glass former can retain a liquid-like free surface even though its bulk may well have vitrified^{1–7}. Of films with free surfaces, a reduction in the glass transition temperature T_g accompanied by accelerated structural relaxation near the surface region has been observed^{8–12}. Such surface-enhanced dynamics is confined to a surface mobile layer, over which local structural relaxation is accelerated. Its thickness has been studied in experiments^{13–15} and simulations^{16–21}. However, estimated values of the thickness and its temperature dependence can vary significantly among different definitions and are not yet fully understood.

A deeper question concerns the mechanism of the enhanced dynamics and the spatial functional form of its penetration into the interior of a film. It was argued that the local structural relaxation time, i.e. α -relaxation time, $\tau_\alpha(z)$ can shed light on the general question of the glass transition^{22–29}. Here z is the depth from the free surface of a film. Yet, direct experimental tests of local properties against theoretical predictions are technically difficult, given the limited spatial resolution^{23,30}. Recently, accurate measurements of $\tau_\alpha(z)$ from molecular dynamics (MD) simulations are reported to support a double-exponential form with an exponential-of-power-law tail given by²⁸

$$\tau_\alpha^{-1}(z) = (\tau_\alpha^{\text{bulk}})^{-1} \exp[a \exp(-z/\xi_0) + b/z], \quad (1)$$

more often written as

$$\ln(\tau_\alpha^{\text{bulk}}/\tau_\alpha(z)) = a \exp(-z/\xi_0) + b/z, \quad (2)$$

where ξ_0 measures the mobile layer thickness, $\tau_\alpha^{\text{bulk}}$ is the bulk α -relaxation time, and a and b are constants. Based on an elastically cooperative nonlinear Langevin equation (ECNLE) theory²⁶, the double-exponential term, found also in early MD simulations³¹, can be derived from an empirical layer-by-layer facilitation-like process for surface effects, while the tail can follow from a local softening due to an elastic coupling in three dimensions to the free surface²⁸. Although the power-law tail covers only half a decade of scaling and may require further scrutiny, the intriguing two-component form seems evident from the accurate MD results. The functional form of Eq. (2) was claimed as a unique signature for the relevance of elastic field in glass²⁸. This echoes a recent increase of interest^{32,33} in the possible dominating role of elasticity in glassy dynamics^{34,35}.

Lattice models of glass in general enjoy superior computational efficiency^{36,37}. Here we use a distinguishable particle lattice model (DPLM)^{38,39} to study the relaxation dynamics of supported glassy films. The DPLM is fundamentally a free-volume model. It generalize multi-species model for glass. Emergent facilitation is seen without explicit facilitation rules. The DPLM has been able to reproduce a variety of characteristic phenomena for bulk samples of glass, including slow relaxation³⁸, Kovacs paradox⁴⁰ and effect⁴¹, kinetic and thermodynamic fragility³⁹, heat capacity overshoot⁴², two-level systems⁴³, diffusion coefficient power-laws⁴⁴, and Kauzmann's paradox⁴⁵. The same model has also successfully simulated surface enhanced mobility⁴⁶ and heat capacity⁴⁷ of glassy films. The importance of adopting an extensively tested lattice model is to ensure compatibility among explanations of a wide range of glassy phenomena. Mechanisms considered in this study based on the DPLM are thus also consistent with the aforementioned list of characteristics of glass in both bulk and film geometries.

In this paper, we measure and contrast estimates of the

^{a)}yangsen@mail.xjtu.edu.cn

^{b)}yanke@mail.xjtu.edu.cn

^{c)}C.H.Lam@polyu.edu.hk

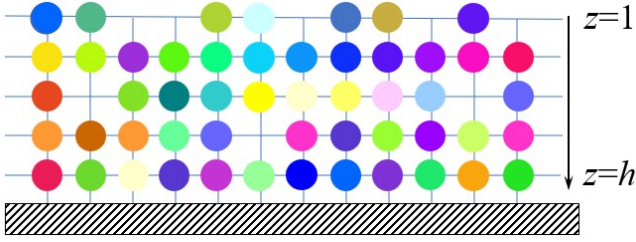


FIG. 1. A schematic drawing of the lattice model of supported film.

thickness of the surface mobile layer from DPLM simulations based on several commonly used definitions. We demonstrate that the local α -relaxation time $\tau_\alpha(z)$ measured for DPLM films can as well be fitted by Eq. (2), despite the absence of elastic effects. Finally, we show that the particle hopping rate from the DPLM admits much weaker surface enhancement than the relaxation time and the implications will be discussed.

II. MODEL

We follow the construction of DPLM films and all model parameters introduced previously for mobility and heat capacity measurements^{46,47}. Specifically, N distinguishable particles of each of their own type populate a square lattice of ribbon geometry, with thickness h and length $L = 1000$, in two dimensions (2D). Each lattice site can be occupied by either a particle or a void (non-occupied), as shown in Fig. 1. We apply periodic boundary conditions along the direction of L and fixed bounding walls along the direction of h . We designate $z = 1$ for the particles in contact with the vacuum represented by the upper wall and $z = h$ for the particles that sit on top of the substrate modeled by the lower wall. The energy of the model is given by

$$E = \sum_{\langle i,j \rangle} V_{s_i s_j} n_i n_j + \epsilon_{\text{bot}} \sum_{i: z_i=h} n_i + \epsilon_{\text{top}} \sum_{i: z_i=1} n_i. \quad (3)$$

Here, the particle type at the site i is labeled s_i . The interaction energy between the particle at the site i and the particle at the adjacent site j is given by $V_{s_i s_j}$. The occupation number $n_i = 1$ at site i if site i is occupied by a particle, otherwise $n_i = 0$ if the site is empty. The z -coordinate (i.e. depth) of site i is given by z_i . We use $\epsilon_{\text{top}} = 1.124$ to account for the excess interfacial energy experienced by particles in $z = 1$ and $\epsilon_{\text{bot}} = -0.5$ for particles in $z = h$, respectively. With the parameters chosen above, it has been shown⁴⁶ that the particle density at $z > 1$ equilibrates at a constant value of 0.99, and drops sharply to 0.2 at $z = 1$. The substrate is then dynamically neutral approximately at the studied temperatures. Notice that the first term of Eq. (3) resembles the definition of a lattice gas model at first glance. The crucial difference is that the pair-interaction energy $V_{s_i s_j}$ takes a random value for particle types s_i and s_j sampled at the beginning of a simulation. This definition introduces a disorder quenched in the configuration space so that the same interaction energy always applies for any given local

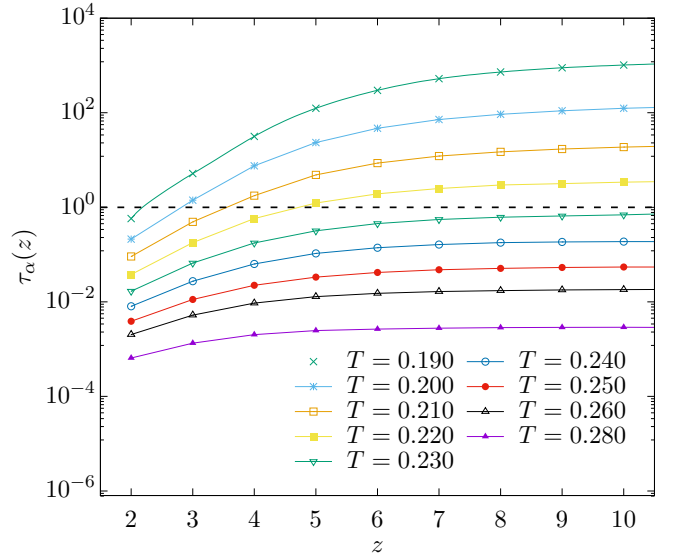


FIG. 2. Structural relaxation time, $\tau_\alpha(z)$, for a film of thickness $h = 45$ at various values of temperature T . The free surface is adjacent to particles at $z = 1$. The dashed line sets an empirical reference observation time $\tau_0 = 1$.

configuration. This ultimately leads to emergent glassy phenomena. We sample $V_{s_i s_j}$ from a *a priori* distribution,

$$g(V) = G_0 / (V_1 - V_0) + (1 - G_0) \delta(V - V_1), \quad (4)$$

where $V_0 = -0.5$, $V_1 = 0.5$ and $G_0 = 0.7$ are parameters chosen for the study⁴⁶. The value of G_0 in Eq. (4) has been demonstrated to control the fragility of glass formers³⁹.

We simulate void-induced equilibrium dynamics with the Metropolis algorithm. The rate for a particle hopping to an adjacent void is given by

$$w = w_0 \exp[-\Delta E \Theta(\Delta E) / k_B T], \quad (5)$$

where ΔE is the energy change due to the hop, $\Theta(\Delta E) = 1$ if $\Delta E > 0$ or $\Theta(\Delta E) = 0$ otherwise. We set the attempt frequency $w_0 = 10^6$. We use $k_B = 1$, so the temperature has the same dimension as energy. The adopted algorithm guarantees detailed balance.

We use the swap algorithm (swapping among all particles and voids) to accelerate the equilibration process^{44,48}. More than 10^5 swap attempts per site are performed to equilibrate the energy and depth-dependent particle density. Before taking measurements, another 10^5 swap attempts per site are performed to confirm that equilibrium has been attained.

III. RELAXATION RATE AND MOBILE LAYER THICKNESS

We measure from DPLM simulations the local overlap function $q(\Delta t, z)$, which gives the probability that a particle in layer z is at the original position after a duration Δt . In

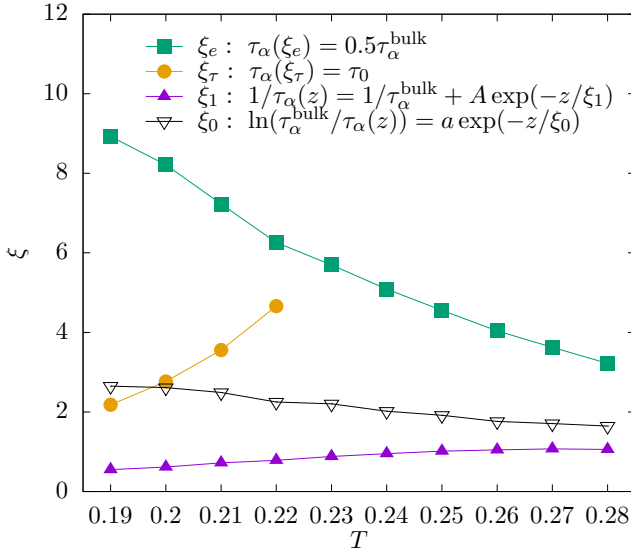


FIG. 3. Thicknesses of surface mobile layer based in different definitions against temperature T for a film of $h = 45$.

Fig. 2, we display the layer-resolved relaxation time $\tau_\alpha(z)$ defined via $q(\Delta t, z) = 1/e$ at $\Delta t = \tau_\alpha(z)$ ⁴⁶. As seen, a slope of $\tau_\alpha(z)$ extends towards the bulk and increases as T is reduced from 0.28 to 0.19. This is consistent with MD simulations¹⁶ and signifies the penetration of fast surface dynamics into the interior of the film.

Using $\tau_\alpha(z)$ from Fig. 2, we calculate the mobile layer thickness ξ_0 from the double-exponential term in Eq. (2). Alternatively, we define a different mobile layer thickness ξ_τ according to^{14,18,27},

$$\tau_\alpha(\xi_\tau) = \tau_0, \quad (6)$$

based on an empirical reference relaxation time τ_0 . We have used $\tau_0 = 1$. Beyond the length scale set by ξ_τ , the dynamics is considered frozen for a practical observation time τ_0 . It is thus often more relevant in interpreting experimental results¹⁴. In addition, one may introduce a third definition of thickness ξ_e according to^{17,18,20}

$$\tau_\alpha(\xi_e) = 0.5\tau_\alpha^{\text{bulk}}, \quad (7)$$

where the mobility enhancement is gauged by the empirical prefactor 0.5 for the reduction of the relaxation time from the bulk value $\tau_\alpha^{\text{bulk}}$. Such a definition then quantifies the width with dynamics significantly faster than the bulk dynamics. Finally, from the gradient of $\tau_\alpha(z)$ close to the free surface, we define a width ξ_1 by a single-exponential form²¹

$$\tau_\alpha(z)^{-1} = (\tau_\alpha^{\text{bulk}})^{-1} + Ae^{-z/\xi_1}. \quad (8)$$

Both ξ_0 and ξ_1 quantify the characteristic decay lengths in the convergence of depth-resolved relaxation rate to its bulk value, according to different functional forms assumed by Eq. (2) and Eq. (8) respectively.

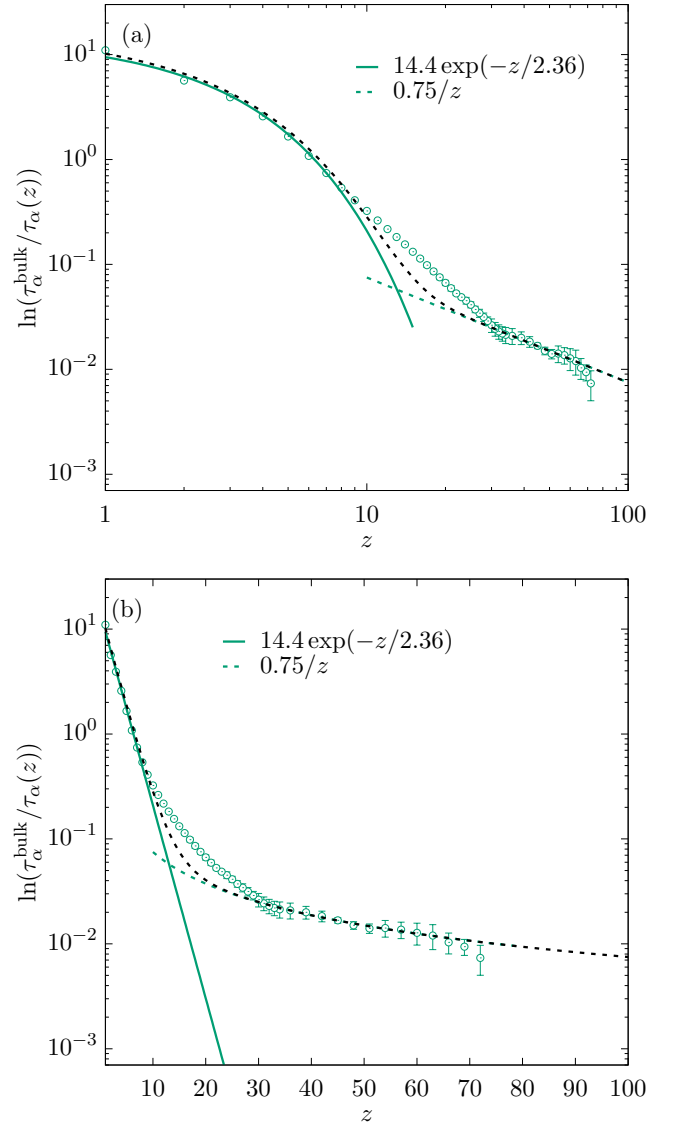


FIG. 4. Plot of $\ln(\tau_\alpha^{\text{bulk}}/\tau_\alpha(z))$ versus depth z in (a) log-log and (b) semi-log scales for a film of thickness $h = 100$ at $T = 0.21$. Two asymptotic fits to the data are also displayed. The black line indicates the sum of the two fits.

Figure 3 plots DPLM results on the thicknesses described above. As temperature decreases, we observe that ξ_τ and ξ_1 decrease while ξ_0 and ξ_e increase. The temperature dependence of ξ_τ , ξ_0 , and ξ_e has been studied before. Specifically, experiments on ξ_τ ¹⁴ and MD results on ξ_τ ¹⁸, ξ_0 ³¹ and ξ_e ^{17,18,20} have all reported trends in good agreement with those from the DPLM in Fig. 3.

We have measured surface mobile layer thicknesses ξ_0 , ξ_τ , ξ_e , and ξ_1 defined in Eqs. (2), (6), (7), and (8) respectively. Our results show that ξ_τ and ξ_1 increase with temperature, while ξ_0 and ξ_e decrease with temperature. Such opposite trends are consistent with previous studies as explained above and have been discussed based on Adam-Gibbs theory¹⁸ and cooperative free volume theory²⁷. The reproduc-

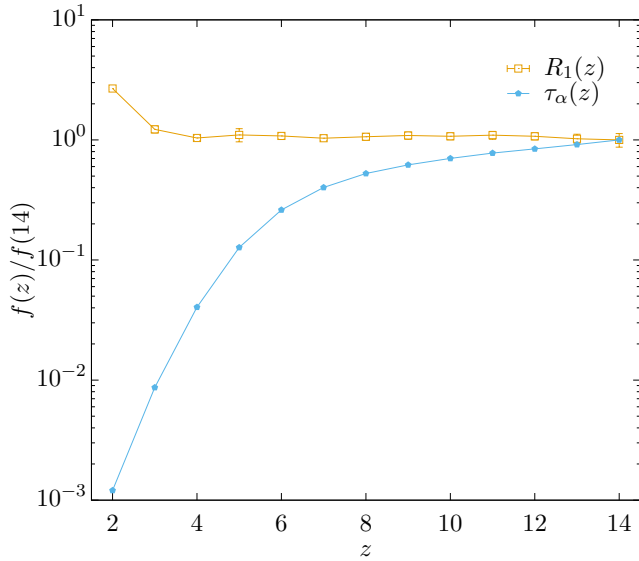


FIG. 5. Particle hopping rate $R_1(z)$ against depth z for a film of thickness $h = 15$ at temperature $T = 0.20$. Also plotted is structural relaxation time $\tau_\alpha(z)$ under the same conditions. The data is normalized by the respective quantity at $z = 14$.

tion of these trends here further supports the applicability of the DPLM on surface-enhanced dynamics in glassy films^{46,47}, in addition to several other glassy phenomena demonstrated previously^{39–45}.

The different properties of the various thicknesses demonstrate that a full characterization of surface enhanced mobility in general requires the whole function of layer-resolved relaxation time $\tau_\alpha(z)$, while an individual thickness reflects only certain features of the dynamics. In particular, ξ_e captures the length scale over which the system cannot maintain its bulk dynamics. It may be most closely related to the dynamic correlation length of glass in bulk, which is expected to increase as temperature decreases. In contrast, ξ_l is a decay length of enhanced dynamics close to the surface. It dictates the length scale of the layer dominating surface flow and is thus most relevant for quantifying surface transport^{10,19}. Its value decreases as temperature decreases, signifying that transport is dominated by an increasingly thinner layer.

To further analyze the functional form of $\tau_\alpha(z)$, we have measured $\tau_\alpha(z)$ from supported DPLM films of thickness $h = 100$. We determine $\tau_\alpha^{\text{bulk}}$ accurately from simulations of bulk samples so that statistical errors are dominated by those of $\tau_\alpha(z)$. Figure 4 plots $\log(\tau_\alpha^{\text{bulk}}/\tau_\alpha(z))$ against z . The result strikingly resembles those from recent MD measurements²⁸ and can be reasonably fitted to Eq. (2) with a double-exponential form in the short range and an upward-turning tail at $z \gtrsim 30$.

IV. WEAK SURFACE EFFECTS ON PARTICLE HOPS

Despite strong surface effects on the relaxation time, we next show that they are much weaker on particle hopping rate.

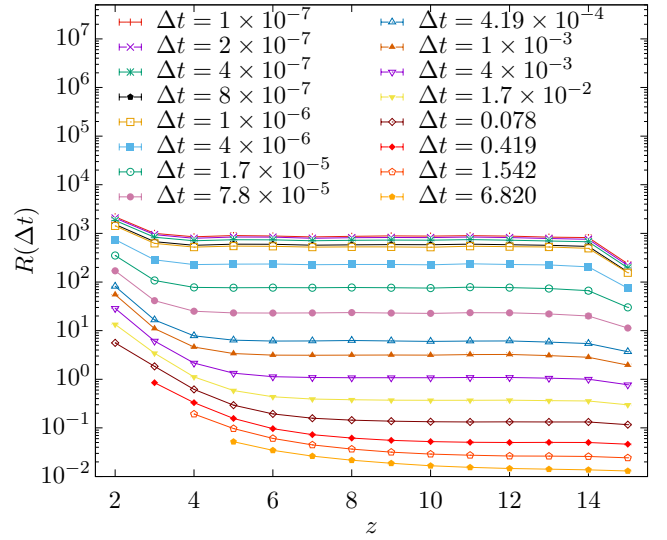


FIG. 6. Net hopping rates $R(\Delta t)$ against depth z for a film of thickness $h = 15$ at different values of Δt at $T = 0.20$.

At deep supercooling, particle dynamics in glass formers are dominated by activated particle hops as revealed by the emergence of secondary and higher-order peaks in the van Hove correlation function⁴⁹. We now analyze the particle hopping rate defined by²¹,

$$R_1(z) = \frac{P_{\text{hop}}(\Delta t, z)}{\Delta t}. \quad (9)$$

Here, $P_{\text{hop}}(\Delta t, z)$ denotes the probability that a particle at layer z hops during a time interval Δt and is given by

$$P_{\text{hop}}(\Delta t, z) = \langle \Theta(|\mathbf{r}_i(t + \Delta t) - \mathbf{r}_i(t)| - 1) \rangle_{t,z}, \quad (10)$$

where $\Theta(x) = 1$ if $x \geq 0$, $\mathbf{r}_i(t)$ is the position of particle i at time t and the average is taken over time t and all the particles that reside at depth z at the beginning of the time interval. We take a small time interval $\Delta t = 10^{-7}$ so that $R_1(z)$ measures the rate of all particle hops.

Our main result on particle hops is shown in Figure 5 which displays $R_1(z)$ measured against z from DPLM simulations at a low temperature of $T = 0.20$. It is compared with $\tau_\alpha(z)$ reported above and values have been normalized by their approximate bulk values taken at $z = 14$. A clear difference between the strengths of the surface effects is seen. Specifically, $\tau_\alpha(z)$ forms a gradient penetrating deep into the interior of the film up to at least $z \simeq 13$. In contrast, a gradient in $R_1(z)$ extends only up to $z \simeq 3$.

To justify that time duration $\Delta t = 10^{-7}$ used in measuring $R_1(z)$, we next describe more comprehensive results based on other values of Δt . Following a definition applied previously to MD results²¹, we generalize Eq. (9) to a net hopping rate $R(z, \Delta t) = P_{\text{hop}}(\Delta t, z)/\Delta t$. In particular, for the very small time interval $\Delta t = 10^{-7}$ used above, the hopping rate $R_1(z)$ is restored. Figure 6 plots results on $R(z, \Delta t)$ for different Δt from DPLM simulations. Note that we have ensured that Δt is small enough by showing only data points

for which $P_{\text{hop}}(\Delta t, z) \leq 0.5$. The results in Fig. 6 qualitatively resemble those from MD simulations²¹. For $\Delta t \simeq 10^{-7}$, $R(z, \Delta t) \simeq R_1(z)$ have approximately converged and this signifies that all hops are properly counted. In contrast, $R(z, \Delta t)$ decreases with Δt at larger Δt . This is because back-and-forth hops, which are very abundant in the system, then do not contribute to $R(z, \Delta t)$, highlighting that they also do not contribute to the net dynamics at longer time scales as explained in²¹. In particular, the gradient in $R(z, \Delta t)$ penetrates deeper into the bulk for larger Δt . More precisely, $R(z, \Delta t)$ at $\Delta t = 6.820$ converges to its bulk value at $z \gtrsim 12$, in sharp contrast to $R_1(z)$ which converges at a much shallower depth of $z \gtrsim 3$. This exemplifies that surface effects for long-time measurements such as $R(z, \Delta t)$ for large Δt and $\tau_\alpha(z)$ penetrate deeper than short-time values such as $R_1(z)$ ²¹.

V. DISCUSSIONS

The ECNLE theory based on elastic interactions³⁵ is an insightful analytical approach used in deriving Eq. (2), providing extensive microscopic details essential for close comparisons with MD simulations and other descriptions of glass relaxation. The exponential-of-power-law tail was taken as a unique signature of a long-range elastic field²⁸. The fact that it is seen in Fig. 4 for the DPLM without elasticity calls into question such a feature as decisive evidence for the elastic picture.

Both the DPLM and the ECNLE theory can account for the exponential-of-power-law tail in the relaxation time, but they essentially produce opposite predictions on the particle hopping rate. The DPLM results on hopping rates reported above are in good qualitative agreement with our MD simulations on free-standing polymer films reported in Ref. 21. In the MD study, we have identified a peculiar layer, referred to as the inner-surface layer, which exhibits a bulk-like particle hopping rate $R_1(z)$ but a surface enhanced mobility as revealed from long-time net hopping rate $R(z, \Delta t)$. Despite only about three particle diameters thick, its existence including its two apparently contradictory defining features is evident. The DPLM, as observed from Fig. 5, also exhibits such an inner surface layer and is located at $3 \lesssim z \lesssim 13$. The thickness is much more pronounced, presumably due to measurement of enhanced mobility based on $\tau_\alpha(z)$ and the thicker film used. Deeper supercooling is expected to increase the thickness of the inner surface layer for both MD and DPLM.

A natural reason for the bulk-like hopping rate is bulk-like particle hopping energy barriers in the inner surface layer²¹. The close proximity of the inner surface layer to the surface region with a reduced density, which is only four particle diameters away in the MD simulations, implies that particle hops are very localized events depending only on molecular arrangements in the immediate neighborhood. Thus, barriers dominated by long-range interactions such as elasticity may not be applicable, as argued in Ref. 21. The short-range nature of the interactions in Eq. (3) for the DPLM is crucial for the convergence of the hopping rate to the bulk value already $z \simeq 3$ as shown in Fig. 5. Note that the dynamics in lattice

models with elasticity can be simulated accurately and rather efficiently and particle hopping rates are well-known to depend non-trivially on morphological features and composition at a distance⁵⁰.

In contrast, the ECNLE theory analyzes dynamics dictated by particle activated hopping energy barriers³⁵. Long-range elasticity introduces a term in the hopping barrier which decays spatially as a power law from the free surface. The structural relaxation rate is then follows from the barrier via a standard Arrhenius relation for activated processes. This relaxation rate is essentially also the particle hopping rate which must also follow the same Arrhenius relation. Therefore, one should predict surface effects on relaxation rate penetrating as deep as those on hopping rates. It is not clear how the ECNLE theory can be reconciled with MD results in Ref. 21.

Back-and-forth motions are known to be important in glassy materials^{51,52}. The deeper penetration of surface effects on relaxation time in the inner surface layer has been attributed to a breakdown of such back-and-forth hopping tendency close to the free surface via facilitation²¹. The DPLM exhibits strongly back-and-forth motions at deep supercooling³⁸ and can demonstrate enhanced mobility when those anti-correlations are reduced close to the surface. In contrast, hopping correlation is completely neglected in the ECNLE theory³⁵. In its present form, it has implemented no mechanism to distinguish between structural relaxation rate and particle hopping rate.

Enhanced mobility has been suggested to propagate into the film via stringlike motions originating from close to the free surface, as revealed by particle trajectory from MD simulations²¹. Similar facilitation via stringlike motions is also observed from particle displacement profiles in DPLM simulations⁴⁶. Assuming that stringlike motions are induced by a fragmented form of voids called quasivoids⁵³, we believe that void-induced facilitation accounts for the surface enhanced mobility in glassy films, as illustrated by the DPLM.

To conclude, we have measured from DPLM simulations the temperature dependence of four definitions of surface mobile layer thickness in glassy films. Different trends are observed in agreement with previous studies and they follow from different characteristics of the layer-resolved relaxation time. We also study the relaxation time including regions deep into the film. A two-component form with a slowly decaying tail closely resembling accurate MD measurements is observed. Our results show that long-range elastic interactions, which are absent in the DPLM, are not a necessary explanation of the tail. We also demonstrate that the particle hopping rate admits much shallower surface effects in the DPLM, again in agreement with MD simulations. It has been shown the dynamics is qualitatively similar for the 2D- and 3D-DPLM in bulk geometries⁵⁴. We thus anticipate that the conclusions drawn from the current results of 2D simulations remain valid in 3D.

ACKNOWLEDGMENTS

This work was supported by China Postdoc Fund Grant No. 2022M722548, Shaanxi NSF Grant No. 2023-JC-QN-0018, Central University Basic Research Fund Grant No. xzy012023044, National Natural Science Foundation of China Grant No. 12405042, Hong Kong GRF Grant No. 15303220.

DATA AVAILABILITY STATEMENT

The data that support the findings of this study are available from the corresponding author upon reasonable request.

- ¹J. Baschnagel and F. Varnik, "Computer simulations of supercooled polymer melts in the bulk and in confined geometry," *Journal of Physics: Condensed Matter* **17**, R851 (2005).
- ²M. D. Ediger and J. A. Forrest, "Dynamics near free surfaces and the glass transition in thin polymer films: a view to the future," *Macromolecules* **47**, 471 (2013).
- ³S. Napolitano, E. Glynos, and N. B. Tito, "Glass transition of polymers in bulk, confined geometries, and near interfaces," *Reports on Progress in Physics* **80**, 036602 (2017).
- ⁴G. B. McKenna and S. L. Simon, "50th anniversary perspective: Challenges in the dynamics and kinetics of glass-forming polymers," *Macromolecules* **50**, 6333–6361 (2017).
- ⁵C. B. Roth, "Polymers under nanoconfinement: where are we now in understanding local property changes?" *Chemical Society Reviews* **50**, 8050 (2021).
- ⁶C. Rodriguez-Tinoco, M. Gonzalez-Silveira, M. A. Ramos, and J. Rodriguez-Viejo, "Ultrastable glasses: new perspectives for an old problem," *La Rivista del Nuovo Cimento* **45**, 325–406 (2022).
- ⁷D. Cangialosi, "Physical aging and vitrification in polymers and other glasses: Complex behavior and size effects," *Journal of Polymer Science* **62**, 1952–1974 (2024).
- ⁸J. L. Keddie, R. A. L. Jones, and R. A. Cory, "Size-dependent depression of the glass transition temperature in polymer films," *Euro. Phys. Lett.* **27**, 59 (1994).
- ⁹Z. Fakhraai and J. A. Forrest, "Measuring the surface dynamics of glassy polymers," *Science* **319**, 600 (2008).
- ¹⁰Z. Yang, Y. Fujii, F. K. Lee, C.-H. Lam, and O. K. C. Tsui, "Glass transition dynamics and surface layer mobility in unentangled polystyrene films," *Science* **328**, 1676 (2010).
- ¹¹L. Zhu, C. Brian, S. Swallen, P. Straus, M. Ediger, and L. Yu, "Surface self-diffusion of an organic glass," *Physical Review Letters* **106**, 256103 (2011).
- ¹²Y. Chai, T. Salez, J. D. McGraw, M. Benzaquen, K. Dalnoki-Veress, E. Raphaël, and J. A. Forrest, "A direct quantitative measure of surface mobility in a glassy polymer," *Science* **343**, 994 (2014).
- ¹³M. Ilton, D. Qi, and J. A. Forrest, "Using nanoparticle embedding to probe surface rheology and the length scale of surface mobility in glassy polymers," *Macromolecules* **42**, 6851–6854 (2009).
- ¹⁴K. Paeng, S. F. Swallen, and M. D. Ediger, "Direct measurement of molecular motion in freestanding polystyrene thin films," *Journal of the American Chemical Society* **133**, 8444 (2011).
- ¹⁵H. Yuan, J. Yan, P. Gao, S. K. Kumar, and O. K. Tsui, "Microscale mobile surface double layer in a glassy polymer," *Science Advances* **8**, eabq5295 (2022).
- ¹⁶F. Varnik, J. Baschnagel, and K. Binder, "Reduction of the glass transition temperature in polymer films: A molecular-dynamics study," *Physical Review E* **65**, 021507 (2002).
- ¹⁷P. Z. Hanakata, J. F. Douglas, and F. W. Starr, "Local variation of fragility and glass transition temperature of ultra-thin supported polymer films," *The Journal of Chemical Physics* **137**, 244901 (2012).
- ¹⁸R. J. Lang and D. S. Simmons, "Interfacial dynamic length scales in the glass transition of a model freestanding polymer film and their connection to cooperative motion," *Macromolecules* **46**, 9818–9825 (2013).
- ¹⁹C.-H. Lam and O. K. C. Tsui, "Crossover to surface flow in supercooled unentangled polymer films," *Phys. Rev. E* **88**, 042604 (2013).
- ²⁰A. Shavit and R. A. Riggleman, "Physical aging, the local dynamics of glass-forming polymers under nanoscale confinement," *The Journal of Physical Chemistry B* **118**, 9096–9103 (2014), pMID: 25046680.
- ²¹C.-H. Lam, "Deeper penetration of surface effects on particle mobility than on hopping rate in glassy polymer films," *J. Chem. Phys.* **149**, 164909 (2018).
- ²²D. Long and F. Lequeux, "Heterogeneous dynamics at the glass transition in van der Waals liquids, in the bulk and in thin films," *Eur. Phys. J. E* **4**, 371 (2001).
- ²³C. J. Ellison and J. M. Torkelson, "The distribution of glass-transition temperatures in nanoscopically confined glass formers," *Nature Materials* **2**, 695 (2003).
- ²⁴J. E. Pye, K. A. Rohald, E. A. Baker, and C. B. Roth, "Physical aging in ultrathin polystyrene films: Evidence of a gradient in dynamics at the free surface and its connection to the glass transition temperature reductions," *Macromolecules* **43**, 8296 (2010).
- ²⁵T. Salez, J. Salez, K. Dalnoki-Veress, E. Raphaël, and J. A. Forrest, "Cooperative strings and glassy interfaces," *Proc. Natl. Acad. Sci.* **112**, 8227 (2015).
- ²⁶A. D. Phan and K. S. Schweizer, "Theory of the spatial transfer of interface-nucleated changes of dynamical constraints and its consequences in glass-forming films," *J. Chem. Phys.* **150** (2019).
- ²⁷R. P. White and J. E. Lipson, "Dynamics across a free surface reflect interplay between density and cooperative length: Application to polystyrene," *Macromolecules* **54**, 4136 (2021).
- ²⁸A. Ghanekarade, A. D. Phan, K. S. Schweizer, and D. S. Simmons, "Signature of collective elastic glass physics in surface-induced long-range tails in dynamical gradients," *Nat. Phys.* **19**, 800 (2023).
- ²⁹C. Herrero and L. Berthier, "Direct numerical analysis of dynamic facilitation in glass-forming liquids," *Phys. Rev. Lett.* **132**, 258201 (2024).
- ³⁰R. R. Baglay and C. B. Roth, "Experimental study of the influence of periodic boundary conditions: Effects of finite size and faster cooling rates on dissimilar polymer–polymer interfaces," *ACS Macro Letters* **6**, 887 (2017).
- ³¹P. Scheidler, W. Kob, and K. Binder, "The relaxation dynamics of a confined glassy simple liquid," *The European Physical Journal E* **12**, 5 (2003).
- ³²A. Tahaei, G. Biroli, M. Ozawa, M. Popović, and M. Wyart, "Scaling description of dynamical heterogeneity and avalanches of relaxation in glass-forming liquids," *Phys. Rev. X* **13**, 031034 (2023).
- ³³M. R. Hasyim and K. K. Mandapapu, "Emergent facilitation and glassy dynamics in supercooled liquids," *Proceedings of the National Academy of Sciences* **121**, e2322592121 (2024).
- ³⁴J. C. Dyre, "Colloquium: The glass transition and elastic models of glass-forming liquids," *Rev. Mod. Phys.* **78**, 953 (2006).
- ³⁵K. S. Schweizer and D. S. Simmons, "Progress towards a phenomenological picture and theoretical understanding of glassy dynamics and vitrification near interfaces and under nanoconfinement," *J. Chem. Phys.* **151**, 240901 (2019).
- ³⁶J. P. Garrahan, P. Sollich, and C. Toninelli, "Kinetically constrained models," in *Dynamical Heterogeneities in Glasses, Colloids and Granular Media*, edited by L. Berthier, G. Biroli, J.-P. Bouchaud, L. Cipelletti, and W. van Saarloos (Oxford University Press, 2011).
- ³⁷F. Ritort and P. Sollich, "Glassy dynamics of kinetically constrained models," *Adv. Phys.* **52**, 219 (2003).
- ³⁸L.-H. Zhang and C.-H. Lam, "Emergent facilitation behavior in a distinguishable-particle lattice model of glass," *Phys. Rev. B* **95**, 184202 (2017).
- ³⁹C.-S. Lee, M. Lulli, L.-H. Zhang, H.-Y. Deng, and C.-H. Lam, "Fragile glasses associated with a dramatic drop of entropy under supercooling," *Phys. Rev. Lett.* **125**, 265703 (2020).
- ⁴⁰M. Lulli, C.-S. Lee, H.-Y. Deng, C.-T. Yip, and C.-H. Lam, "Spatial heterogeneities in structural temperature cause Kovacs' expansion gap paradox in aging of glasses," *Phys. Rev. Lett.* **124**, 095501 (2020).
- ⁴¹M. Lulli, C.-S. Lee, L.-H. Zhang, H.-Y. Deng, and C.-H. Lam, "Kovacs effect in glass with material memory revealed in non-equilibrium particle interactions," *J. Stat. Mech.* **2021**, 093303 (2021).

- ⁴²C.-S. Lee, H.-Y. Deng, C.-T. Yip, and C.-H. Lam, “Large heat-capacity jump in cooling-heating of fragile glass from kinetic monte carlo simulations based on a two-state picture,” *Phys. Rev. E* **104**, 024131 (2021).
- ⁴³X.-Y. Gao, H.-Y. Deng, C.-S. Lee, J. You, and C.-H. Lam, “Emergence of two-level systems in glass formers: a kinetic monte carlo study,” *Soft Matter* **18**, 2211 (2022).
- ⁴⁴G. Gopinath, C.-S. Lee, X.-Y. Gao, X.-D. An, C.-H. Chan, C.-T. Yip, H.-Y. Deng, and C.-H. Lam, “Diffusion-coefficient power laws and defect-driven glassy dynamics in swap acceleration,” *Phys. Rev. Lett.* **129**, 168002 (2022).
- ⁴⁵X.-Y. Gao, C.-Y. Ong, C.-S. Lee, C.-T. Yip, H.-Y. Deng, and C.-H. Lam, “Kauzmann paradox: A possible crossover due to diminishing local excitations,” *Phys. Rev. B* **107**, 174206 (2023).
- ⁴⁶Q. Zhai, X.-Y. Gao, C.-S. Lee, C.-Y. Ong, K. Yan, H.-Y. Deng, S. Yang, and C.-H. Lam, “Surface mobility gradient and emergent facilitation in glassy films,” *Soft matter* **20**, 4389–4394 (2024).
- ⁴⁷Q. Zhai, X.-Y. Gao, H.-Y. Deng, C.-S. Lee, S. Yang, K. Yan, and C.-H. Lam, “Heat capacity and relaxation dynamics of glassy films: A lattice model study,” *Phys. Rev. E* **111**, 015406 (2025).
- ⁴⁸A. Ninarello, L. Berthier, and D. Coslovich, “Models and algorithms for the next generation of glass transition studies,” *Phys. Rev. X* **7**, 021039 (2017).
- ⁴⁹T. Kawasaki and A. Onuki, “Slow relaxations and stringlike jump motions in fragile glass-forming liquids: Breakdown of the stokes-einstein relation,” *Phys. Rev. E* **87**, 012312 (2013).
- ⁵⁰C.-H. Lam, C.-K. Lee, and L. M. Sander, “Competing roughening mechanisms in strained heteroepitaxy: a fast kinetic monte carlo study,” *Phys. Rev. Lett.* **89**, 216102 (2002).
- ⁵¹K. Vollmayr-Lee, “Single particle jumps in a binary lennard-jones system below the glass transition,” *J. Chem. Phys.* **121**, 4781 (2004).
- ⁵²C.-H. Lam, “Repetition and pair-interaction of string-like hopping motions in glassy polymers,” *J. Chem. Phys.* **146**, 244906 (2017).
- ⁵³C.-T. Yip, M. Isobe, C.-H. Chan, S. Ren, K.-P. Wong, Q. Huo, C.-S. Lee, Y.-H. Tsang, Y. Han, and C.-H. Lam, “Direct evidence of void-induced structural relaxations in colloidal glass formers,” *Phys. Rev. Lett.* **125**, 258001 (2020).
- ⁵⁴B. Li, C.-S. Lee, X.-Y. Gao, H.-Y. Deng, and C.-H. Lam, “The distinguishable-particle lattice model of glasses in three dimensions,” *Soft Matter* **20**, 1009–1017 (2024).